

www.acsabm.org Article

Cell-Free Synthesis of a Transmembrane Mechanosensitive Channel Protein into a Hybrid-Supported Lipid Bilayer

Zachary A. Manzer, Surajit Ghosh, Miranda L. Jacobs, Srinivasan Krishnan, Warren R. Zipfel, Miguel Piñeros, Neha P. Kamat,* and Susan Daniel*



Cite This: ACS Appl. Bio Mater. 2021, 4, 3101–3112



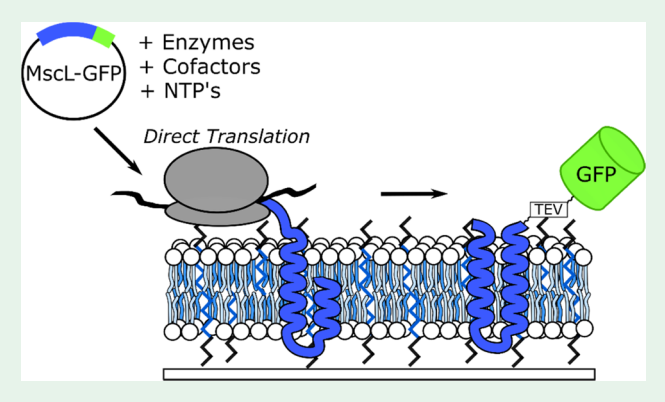
ACCESS

Metrics & More



SI Supporting Information

ABSTRACT: Supported lipid bilayers (SLBs) hold tremendous promise as cellular-mimetic structures that can be readily interfaced with analytical and screening tools. The incorporation of transmembrane proteins, a key component in biological membranes, is a significant challenge that has limited the capacity of SLBs to be used for a variety of biotechnological applications. Here, we report an approach using a cell-free expression system for the cotranslational insertion of membrane proteins into hybrid-supported lipid bilayers (HSLBs) containing phospholipids and diblock copolymers. We use cell-free expression techniques and a model transmembrane protein, the large conductance mechanosensitive channel (MscL), to demonstrate two routes to integrate a channel protein into a HSLB. We show that HSLBs can be assembled with integrated



membrane proteins by either cotranslational integration of protein into hybrid vesicles, followed by fusion of these proteoliposomes to form a HSLB, or preformation of a HSLB followed by the cell-free synthesis of the protein directly into the HSLB. Both approaches lead to the assembly of HSLBs with oriented proteins. Notably, using single-particle tracking, we find that the presence of diblock copolymers facilitates membrane protein mobility in the HSLBs, a critical feature that has been difficult to achieve in pure lipid SLBs. The approach presented here to integrate membrane proteins directly into preformed HSLBs using cell-free cotranslational insertion is an important step toward enabling many biotechnology applications, including biosensing, drug screening, and material platforms requiring cell membrane-like interfaces that bring together the abiotic and biotic worlds and rely on transmembrane proteins as transduction elements.

KEYWORDS: supported lipid bilayer, cell-free protein synthesis, transmembrane proteins, lipids, diblock copolymers, hybrid vesicle

■ INTRODUCTION

The assembly of cellular-mimetic membranes containing functional, oriented membrane proteins remains a longstanding goal of biologists, biophysicists, and engineers alike. This is because the ability to harness membrane proteins, with their exquisite sensitivity, precise molecular recognition, and specific transport capabilities, and assemble them into material interfaces has significant potential for the structural and functional assessment of membrane proteins as well as biotechnological and pharmaceutical applications. Materials made from membrane components have led to the design of biosensors, gene sequencers, and platforms to screen pharmacological drug candidates. 1-3 Nowhere has this goal been more closely achieved than with supported lipid bilayers (SLBs), planar lipid membranes that can interface with electronic, 4,5 optical, 6-8 and spectroscopic systems 9,10 to enable biological activity to be detected and transduced into measurable readouts.

SLBs can be readily assembled on solid surfaces by a number of convenient methods from liposome fusion, 11 Langmuir—

Blodgett—Schaeffer transfer,¹² or solvent-assisted lipid bilayer formation.¹³ Due to their planar geometry, SLBs are compatible with various surface-sensitive characterization and analytical tools, including quartz crystal microbalance with dissipation (QCM-D),¹⁴,¹⁵ surface plasmon resonance,¹⁰ atomic force microscopy,^{10,14},¹⁶ electrochemical impedance spectroscopy,^{4,5} and fluorescence microscopy.¹⁷ The stability of SLBs (owing to the solid support) and their compatibility with various analytical techniques make them popular and convenient model biomembrane surfaces.^{18,19}

Incorporating functional membrane proteins that are both oriented and mobile into SLBs, however, has been a significant challenge that has limited the full application of SLBs as

Received: November 16, 2020 Accepted: February 19, 2021 Published: March 18, 2021





biosensors or biophysical platforms. Typically, membrane proteins are integrated into SLBs using detergent-mediated reconstitution processes to first assemble proteoliposomes followed by liposomal rupture to form a SLB. This type of approach has limitations because either the proteoliposomes are too stiff to rupture or the vesicles are incompatible with the surface to foster rupture. Furthermore, the detergents used to assemble proteoliposomes will inevitably end up in the resulting SLB, changing the membrane composition and properties in unexpected ways. An alternative method is to extract cell blebs from the plasma membrane surfaces and induce their rupture into a planar bilayer. This method, too, has drawbacks, especially for applications where the complexity of plasma membrane would confound investigations into a single protein or where the properties of the membrane need to be tightly controlled. Thus, there is a need for a new approach to integrate folded transmembrane proteins into supported bilayers of controlled compositions while maintaining the salient features of lipid and protein mobility and protein orientation in the membrane.

Cell-free protein synthesis (CFPS) is a relatively new approach that enables the integration of membrane proteins into model biological membranes without typical constraints. 22,23 An important requirement of CFPS is a suitable membrane environment, which is necessary for the proper folding of protein molecules.^{24,25} So far, the cotranslational integration of membrane proteins into synthetic scaffolds has been demonstrated extensively using liposomes and polymersomes in solution or tethered to a surface.² adapt this system to be compatible with SLBs requiring a planar geometry, we set out to explore how a cell-free expression system could be leveraged for the cotranslational insertion of membrane proteins into a supported lipid bilayer while maintaining lipid and protein mobility. Specifically, to address the goals of achieving protein mobility in SLBs, we investigated how the incorporation of diblock copolymers into lipid membranes would affect protein properties. The membrane properties of SLBs containing different phospholipids and diblock copolymers have been reported in the literature; 31-33 however, biotechnological applications using the cotranslational insertion of a membrane protein directly into hybrid SLBs (HSLBs) using cell-free methods, to our knowledge, have never been shown.

Here, we present the use of CFPS to incorporate a membrane protein into a HSLB using two complementary approaches that offer flexibility in reaction conditions and desired surfaces depending on the intended application. We observe that both methods result in oriented proteins and that these proteins are mobile in HSLBs above a certain diblock copolymer concentration, overcoming significant limitations of previous methods of protein-integrated SLBs. The ability to create a HSLB with proteins expressed in a cell-free manner unlocks a wide variety of applications from basic biophysics to biotechnology that is otherwise difficult to attain by traditional methods.

■ EXPERIMENTAL SECTION

Materials. 1,2-Dioleoyl-sn-glycero-3-phosphocholine (DOPC) and poly(ethylene oxide)-b-polybutadiene (PEO₁₄-b-PBD₂₂, 1800 kDa) were obtained from Avanti Polar Lipids (Alabaster, AL) and Polymer Source Inc. (Montreal, Quebec, Canada), respectively. Texas Red 1,2-dihexadecanoyl-sn-glycero-3-phosphoethanolamine, triethylammonium salt (TR-DHPE) was obtained from Thermo Fisher

Scientific. Phosphate-buffered saline (PBS) and Sepharose 4B were obtained from Sigma-Aldrich (St. Louis, MO). Octadecyl rhodamine (R18) was purchased from Molecular Probes (Eugene, OR). All chemicals were used without further purification.

Plasmid Information. pET19b-EcMscL-mEGFP has been described previously.^{2.5} Briefly, a monomeric enhanced green fluorescent protein (mEGFP) is fused to the C-terminal of the *Escherichia coli* mechanosensitive channel of large conductance (EcMscL) under the T7 promoter for cell-free protein expression. A tobacco etch virus (TEV) protease cleavage site is located between MscL and GFP to allow for postexpression GFP removal.

Small Unilamellar Vesicle (SUV) Preparation. Small unilamellar vesicles (SUVs) with varying mol % DOPC and PEO₁₄-b-PBD₂₂ were prepared using thin-film hydration methods.³⁴ Briefly, required amounts of DOPC in CHCl₃ and PEO₁₄-b-PBD₂₂ in CH₂Cl₂ were mixed together in glass vials to achieve the desired mole percentage with a total amphiphile concentration of 5 mM for SLB formation and 26.09 mM for cell-free expression. Excess solvent was evaporated by rotation under a stream of nitrogen to form a lipid film. Films were further dried under vacuum for >4 h to remove trace amounts of solvent. Finally, the films were rehydrated with 300 mOsm PBS (SUVs used for cell-free expression were rehydrated in water instead of PBS) and incubated overnight at 60 °C. The films were then vortexed for several seconds and extruded seven times through a 100 nm nucleopore polycarbonate membrane using an Avanti Mini Extruder (Avanti Polar Lipids, Birmingham, AL).

Characterization of Vesicle Size and Surface Charge. The hydrodynamic size (diameter) and surface charge (ζ potential) of the vesicles in 300 mOsm PBS were measured on a Malvern Instruments Zetasizer Nano-ZS instrument with a 4 mW He–Ne laser ($\lambda=632$ nm) and backscattered detector angle of 173°. The results are summarized in Figure S1, Supporting Information.

Glass Slide Preparation. Microscope cover glass ($25 \times 25 \text{ mm}^2$; no. 1.5; VWR) was cleaned by immersion in a solution containing 70% sulfuric acid (H_2SO_4) and 30% hydrogen peroxide (H_2O_2) for 10 m and then washed under deionized water (18.2 M Ω cm) for 30 m. Just prior to use, the glass slides were dried with a stream of nitrogen and used immediately to assemble supported lipid bilayers.

Supported Lipid Bilayer Formation. Cleaned glass slides were used as solid surfaces for supported lipid bilayer formation. First, poly(dimethylsiloxane) (PDMS, 10:1 elastomer/cross-linker mixture of Sylgard 184) wells (with a diameter of \sim 1 cm) were attached to a cleaned dried glass slide. Then, 80 μ L of each vesicle composition with \sim 0.75 mM concentration was added into the well and incubated for 15–20 min to ensure complete rupture and planar bilayer formation of adsorbed vesicles. After formation, the well was rinsed with PBS to remove excess unruptured vesicles.

Fluorescence Recovery after Photobleaching (FRAP) Measurements. To verify the formation of a fluid-supported lipid bilayer on the glass surface, we monitored fluorescence recovery after photobleaching (FRAP) of fluorescently labeled phospholipids doped into the phospholipid and diblock containing hybrid bilayer films. Approximately 1.0 mol % TR-DHPE was added to all vesicle formulations for the FRAP experiments of vesicle-only samples. For samples containing proteins, we used R18 dye (see the section below).

The instrumental setup for FRAP measurement consists of an inverted Zeiss Axio Observer Z1 microscope with an α Plan-Apochromat 20× objective and 150 mW 561 nm optically pumped semiconductor laser (Coherent, Inc.). After formation of the bilayer, the laser was used to bleach a ~20 μ m diameter spot at the z-plane for 500 ms and then the recovery of the bleached spot's intensity was recorded over 30 min. After background subtraction and normalization for photobleaching effects, fluorescence intensity recovery data was fit to the two-dimensional (2-D) diffusion equation following the method of Soumpasis et al. 35 The following equation was used to calculate the diffusion coefficient (D)

$$D = \frac{w^2}{t_{1/2}} \tag{1}$$

where w and $t_{1/2}$ represent the radius of the photobleached spot and the time required to achieve half of the maximum recovery intensity, respectively.

Quartz Crystal Microbalance with Dissipation (QCM-D) Experiments. QCM-D measurements were performed using a Q-Sense E1 (Biolin Scientific, Sweden) instrument with silicon oxide-coated sensors (QSX 303, Q-Sense) to monitor vesicle adsorption, their rupture process, and bilayer formation. All measurements were performed at ~25.0 °C with a flow rate of 100 μ L/min by a peristaltic pump (Ismatec). First, the surface of each QCM sensor was cleaned by oxygen plasma treatment for 1 min. The PBS buffer was then flowed through the QCM crystal and after obtaining a stable baseline, the vesicle solution was injected. Supported lipid bilayer formation was monitored by recording the change of sensor resonance frequency (ΔF) and energy dissipation (ΔD) with time. The ΔF and ΔD values were observed at the odd overtones (1st–13th). In this article, the reported data were measured at the third overtone and analyzed using Q-tools software (v.3.1.25.604, Nanoscience Instruments).

Cell-Free Protein Synthesis (CFPS). CPFS was performed using the PURExpress In Vitro Protein Synthesis kit from New England Biolabs, Inc. (Ipswich, MA). We followed the manufacturer's protocol for the expression of proteins and supplemented in vesicles to replace $\rm H_2O$ in the reaction mixture or conducted the reaction in the presence of HSLBs. In each reaction, the total reaction volume was 30 $\mu \rm L$ containing PURExpress components, MscL-GFP plasmid (200 ng), and desired vesicles/HSLBs.

During CFPS into vesicles, the concentration of vesicles was kept at \sim 10 mM and the reaction was executed at 37 °C for \sim 2 h. Finally, vesicles were purified by a Sepharose CL-4B column using PBS as the eluent.

For CFPS into HSLBs, we used \sim 0.8 mM vesicles in PBS to form HSLBS prior to the CFPS reaction. After the formation of HSLBs, samples were rinsed with PBS to remove unruptured vesicles and then with autoclaved Milli-Q water to remove excess salts just prior to the addition of the cell-free reaction mixture. CFPS reaction was executed at 37 $^{\circ}$ C for 30–40 min before rinsing the HSLBs with PBS to quench the reaction

Rupture of MscL-GFP-Expressed Vesicles and HSLB Formation. To verify the rupture of proteoliposomes and HSLB formation from them, we labeled MscL-GFP-expressed proteoliposomes with octadecyl rhodamine (R18), a membrane-intercalating fluorescent molecule. We used R18 here instead of Texas Red so that we could postlabel vesicles after protein synthesis prior to HSLB formation. During the labeling of proteoliposomes, 200 µL of MscL-GFP-containing vesicle solution was incubated with 1 μ L of 0.5 mM R18 (dissolved in ethanol), in a sonicating bath (VWR) for 15 min at 4 °C. The labeled MscL-GFP-expressed proteoliposomes in solution were incubated on a treated glass slide for 15 min to form HSLBs. This R18 labeling allowed visual observation of the state of proteoliposomes (i.e., they remain as intact vesicles or rupture to form SLB) using a fluorescence microscope. We conducted similar experiments with protein-free vesicles to compare the lipid diffusion and verify vesicle rupture (as reported by R18) between HSLBs with and without membrane proteins.

Cleavage Assay for Protein Orientation. To determine the orientation of MscL-GFP in the HSLBs, TEV protease (New England Biolabs, Inc.) was used according to manufacturer's recommendations to cleave the GFP molecule from the membrane-bound MscL. Samples were imaged using total internal reflection fluorescence (TIRF) microscopy both before and after overnight incubation with the TEV protease to quantify the loss in fluorescent particles. Samples were covered during incubation to prevent photobleaching, and cleaved GFP molecules were rinsed away using PBS before imaging. Punctate fluorescent particles were counted using Imagel. ³⁶

Characterization of Individual Membrane Protein Motion. To monitor the mobility and orientation of MscL-GFP, supported lipid bilayers containing protein were imaged using total internal reflection fluorescence (TIRF) microscopy on an inverted Zeiss Axio Observer.Z1 microscope with an α Plan-Apochromat 100× objective. A 561 nm solid state laser was used to excite the GFP for tracking. A

Laser TIRF 3 slider (Carl Zeiss, Inc.) was used to control the incident angle to create an evanescent wave of ~ 100 nm. A Semrock LF488-B-ZHE filter cube was used to filter excitation light and to send it to the electron-multiplying charge-coupled device (CCD) camera (Image-EM C9100-13, Hamamatsu). All images were analyzed using ImageJ (NIH) and Matlab (Mathworks). For particle diffusion, we used the slope of the tangent line of the first three points to calculate the local diffusion rate. Particles with a maximum displacement smaller than 50 pixels² were considered immobile, based on immobile fluorescent beads on our microscope. Thotein confinement radius was calculated using eq 2, which is valid for proteins that exhibit confined motion. Note that eached a plateau (indicating confinement), with a mean square displacement of MSD_p.

$$R_{\text{confinement}} = \sqrt{\text{MSD}_{p}}$$
 (2)

Single-Molecule Subunit Counting Microscopy. A lab-built azimuthal-scanning objective-TIRF microscope was used for single-molecule imaging to provide a fully uniformly illuminated field of view. Excitation at 488 nm was directed through a telescope and focusing lens aligned to create a collimated beam out of the objective (Olympus UApoN 100×/1.49), while a pair of XY galvanometer mirrors (model 3210H, Cambridge Technology) scanned the focused beam around the periphery of the objective lens back aperture at ~600 Hz. The TIRF image was collected through an ET525/50 emission filter (Chroma Technology) by an EMCCD (Andor iXon 897 Ultra). Coverslips were scanned for regions with a suitable density of molecules for single-molecule analysis. For bleach step analysis, 2000 frames were typically recorded at 10–30 Hz with the laser intensity kept low to mitigate blinking artifacts.

Single-Molecule Data Analysis. Photobleaching movies were analyzed by a custom lab software package (ImageC.exe, written in C/C++ under Microsoft Visual Studio). Single-molecule spots were located automatically by successive processing of the summed image stack to locate fluorescent puncta above a threshold based on a userspecified Gaussian fit criterion. For each molecule, a region of interest (ROI) (typically 5×5 pixels) centered on the pixel containing the PSF centroid was created and the ROI mean values vs. time (frame) extracted from the stack. Pixel size was 100 nm in the object plane. The ROI center pixel coordinate was readjusted slightly as needed as the data is extracted from the frames so that the brightest pixel is always at the center. The ROI fluorescence traces of all of the spots located were stored within the program and displayed as time trace plots for manual (i.e., visually by the user) step counting or using an automated step-finding algorithm that counts the number of bleach steps based on signal noise and a user-specified change in the trace counts that determines a valid step. Traces without discernible bleach steps were discarded.

■ RESULTS AND DISCUSSION

Hybrid-Supported Lipid Bilayers (HSLBs) Form by Vesicle Fusion and Have Two-Dimensional Lipid Fluidity. We used vesicle fusion to form HSLBs on hydrophilic glass surfaces and fluorescence recovery after photobleaching (FRAP) to confirm vesicle rupture, formation of the planar bilayer, and to measure two-dimensional lipid diffusion within it. To provide an amphiphilic environment to support membrane protein incorporation later, we chose 1,2-dioleoylsn-glycero-3-phosphocholine (DOPC) and the diblock copolymer poly(ethylene oxide)-b-poly(butadiene) (PEO-b-PBD) because these systems are well-characterized and have been shown to positively influence membrane protein expression by providing a tunable amphiphilic environment.²⁵ Additionally, we hypothesized that the hydrophilic PEO group on the diblock copolymer may also provide additional space under the HSLB to promote protein mobility, similar to other polymers,

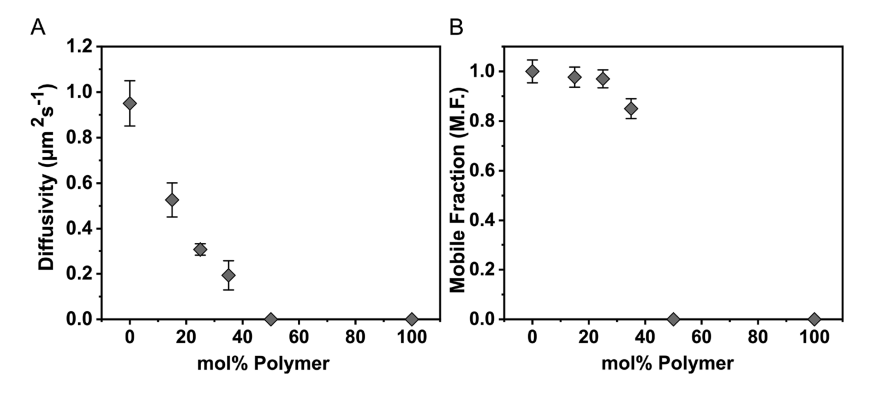


Figure 1. Characterization of HSLB diffusivity (A) and mobile fraction (B), using DOPC and PEO-b-PBD-containing vesicles doped with 1 mol % Texas Red DHPE lipid.

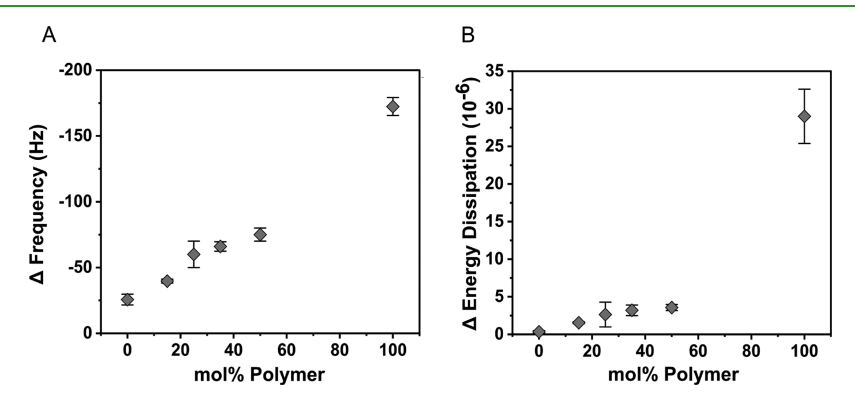


Figure 2. Summary of the overall change in (A) frequency (Hz) and (B) energy dissipation for HSLBs using QCM-D.

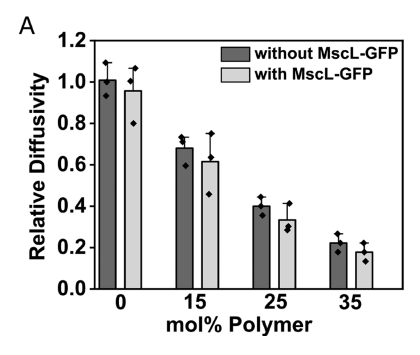
such as polyethylene glycol-conjugated lipids, used to cushion SLBs. $^{41,42}\,$

FRAP experiments were carried out on HSLBs containing a range of lipid-to-diblock copolymer ratios (0-100 mol % PEO-b-PBD) with ~1 mol % TR-DHPE, a fluorescently labeled phospholipid that was used to monitor diffusion. We used vesicles extruded through a 100 nm membrane (see the Supporting Information for size characterization, Figure S1). When placed near a hydrophilic glass surface, these vesicles will readily adsorb to it, which is easily confirmed using fluorescence microscopy. An easy way to determine if those adsorbed vesicles have ruptured into a contiguous planar bilayer is to photobleach the surface and monitor the twodimensional fluorescence recovery over time. In our setup, we photobleach with a laser beam that is $\sim 20 \ \mu m$ in diameter, orders of magnitude larger than a single vesicle, allowing us to interrogate planar bilayer formation on the micron scale. In Figure S2A-F (Supporting Information), we provide images of the fluorescence recovery of the photobleached areas for each vesicle formulation along with the corresponding data and fitted recovery curves. Using these recovery profiles, we calculated the diffusion coefficient (D) of lipid molecules in each HSLB and their corresponding lipid mobile fraction, summarized in Figure 1. Our results indicate that upon photobleaching, HSLBs with 0, 15, 25, and 35 mol % diblock copolymer recovered nearly to full fluorescence in the photobleached region, whereas HSLBs containing 50 or 100 mol % diblock copolymer did not recover, an outcome that happens when the vesicles do not rupture and there is no ability for the photobleached lipids to exchange with those that were not bleached. We observe that as the percentage of the

diblock copolymer is increased, the lipid diffusion coefficient decreases.

There are two possible reasons why the diffusion coefficient decreases as the mole percent of diblock copolymer increases. One possibility is that increasing the concentration of diblock copolymer increases the viscosity of the membrane, ²⁵ and as such, the diffusion coefficient decreases. A second possibility is that increasing the amount of diblock copolymer results in rigid vesicles⁴³ that do not readily rupture to form a bilayer, and thus there are obstacles or defects (e.g., unruptured vesicles or patches) in the bilayer that constrain the diffusive motion. We can rule out this latter possibility by looking at the trend in mobile fraction. For all formulations that are mobile, the mobile fractions are 95% or better. If there was a significant number of unruptured vesicles, the mobile fraction would also decrease. Instead, the relative consistency across the compositions, up to 35 mol %, points to increasing viscosity as the underlying reason for the decreasing diffusion. The observed trends in lipid diffusivity are in good agreement with other lipid and block diblock copolymer SLBs. 31,3

While the photobleaching data supports that a planar bilayer has formed for up to 35 mol % diblock copolymer content, we sought to confirm this with another technique, quartz crystal microbalance with dissipation (QCM-D). The adsorption and rupture of hybrid vesicles on silica surfaces were monitored using QCM-D by measuring changes in resonance frequency (ΔF) and energy dissipation (ΔD). ΔF and ΔD provide information about the adsorbed lipid mass and viscoelastic properties of the adsorbed lipid layer on a silica surface and are useful tools for monitoring the formation of SLBs from vesicles. The addition of DOPC liposomes to the QCM sensor showed characteristic behavior of supported bilayer formation:



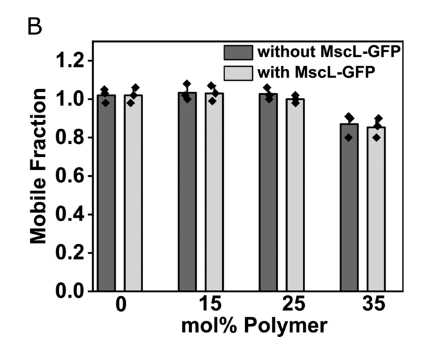


Figure 3. Incorporation of MscL-GFP does not affect lipid diffusivity or mobile fraction. (A) HSLBs with and without MscL-GFP incorporated using cell-free protein synthesis are labeled with R18 to measure lipid diffusivity and mobile fraction. Measurements are relative to 0 mol % diblock copolymer without MscL-GFP. We see the same trend as we observed previously in Figure 1 using Texas Red DHPE as the probe. (B) Overall lipid mobile fraction remains high after protein incorporation.

first, a substantial decrease in sensor frequency and increase in dissipation, owing to the adsorption of intact liposomes to the silica surface, followed by a sharp transition and increase in frequency and decrease in dissipation, which results from the rupture and formation of the planar bilayer film. The signal finally stabilizes with a $\Delta F = \sim 25 \pm 2$ Hz and $\Delta D = \sim 0.2 \times 10^{-6}$ (Figure S3, Supporting Information), a well-known QCM-D response of SLB formation on silica surfaces.

We monitored the QCM-D response of hybrid vesicles with increasing mole percentage of diblock copolymer to assess bilayer formation. A summary of the final ΔF and ΔD is shown in Figure 2. The addition of hybrid vesicles with 15 mol % diblock copolymers also exhibits a typical SLB QCM-D response shape, like DOPC. However, here we see that the kinetics of bilayer formation is apparently a two-step process, with a faster regime initially at the transition point, which then switches over to a slower rise until reaching the final plateau. The two kinetic regimes are mirrored in the dissipation signal as well. These two regimes could result from some vesicles fusing with a more DOPC-like pattern of adsorption then rupture, and those fusing with slower kinetics that are clearly influenced by the diblock copolymer presence. At the plateaus, the overall mass is what we would expect: a shift in frequency due to the diblock copolymer weight, and a shift in dissipation aligning with greater diblock copolymer energy absorption (Figure S3, Supporting Information).

With a further increase in diblock copolymer percentage in DOPC vesicles, a distinct change in QCM-D response is noticed. In 25 mol % diblock copolymer hybrid vesicles, there is initially a sharp decrease followed by a slight increase in frequency, whereas with 35 and 50 mol % diblock copolymer, the sharp decrease is followed by an almost constant frequency. Similarly, in the dissipation profiles, a sharp increase in dissipation, followed by an almost constant value, is observed. We notice that as the mol % diblock copolymer is increased to 50%, the change in frequency and dissipation follow a regular, almost linear, increase of mass, seeming to correspond with the regular addition of mass of the diblock copolymer and its dissipative properties. In contrast, for the 100 mol % diblock copolymer formulation, we found a rapid decrease in frequency and an increase in dissipation, but here the final values of frequency and dissipation were not on the trend and extreme, suggesting only vesicle adsorption on the silica surface with no rupture or bilayer formation.

The fluorescence recovery data and the regularity of the mass and dissipation changes in HSLBs with up to 35 mol %

suggest that the planar bilayer is forming with these amounts of the diblock copolymer in the vesicles. However, the result at 50 mol % diblock copolymer is difficult to interpret. The lack of mobility suggests that vesicles did not rupture, but the change in frequency and dissipation continue to follow the linear trend of the more moderate amounts of polymer. This may suggest that the 50 mol % diblock copolymer vesicles do rupture at least to some extent, although there may still be some unruptured vesicles on the surface.

Cell-Free Expression Methods Enable Incorporation of Oriented Membrane Proteins into HSLBs. We used a cell-free protein synthesis (CFPS) method to incorporate transmembrane proteins into HSLBs. CFPS utilizes either purified synthesis components²⁰ or cellular lysate²¹ to synthesize proteins in vitro from DNA of interest. We used two approaches, each of which makes use of different SLB formation methods to provide flexibility in potential applications that require the incorporation of membrane proteins. In the first approach, we used CFPS to express a transmembrane protein, MscL-GFP, into hybrid vesicles and used vesicle fusion to self-assemble a HSLB containing these transmembrane proteins. In the second approach, we used CFPS to demonstrate the cotranslational insertion of transmembrane proteins directly into preformed HSLBs. We determined that proteins embedded in the HSLB by either approach resulted in a predominant protein orientation, and that the addition of diblock copolymer to HSLBs promoted protein mobility in these HSLBs independent of formation technique.

Approach 1: Proteoliposomes Made from Cell-Free Protein Expression Maintain Lipid Fluidity and Protein Orientation after Rupture to Form Supported Bilayers.

To test that proteoliposomes that incorporate cotranslationally integrated membrane proteins could form a HSLB, we expressed a fluorescently labeled transmembrane ion channel. The large conductance mechanosensitive channel green fluorescent protein fusion (MscL-GFP) was expressed into vesicles containing various amounts of diblock copolymer and vesicles were ruptured postexpression to form bilayers. We analyzed membranes with polymer compositions of 0, 15, 25, 35, 50, and 100 mol % and assessed the capacity of hybrid membranes to form fluid bilayers and fluidize the embedded proteins. To confirm protein expression, we monitored an increase in fluorescence from MscL-GFP.²⁵ GFP not only provides a straightforward way to monitor protein expression,

ACS Applied Bio Materials

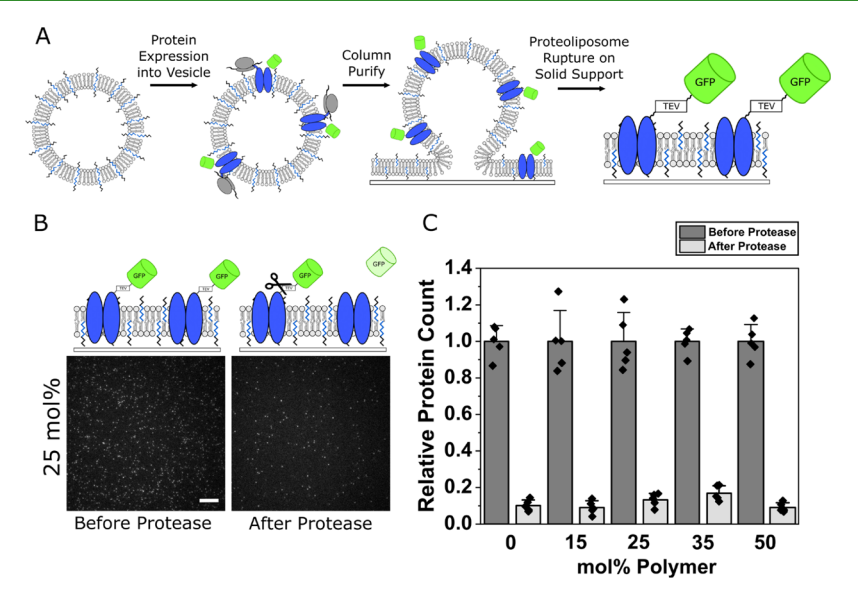


Figure 4. Characterization of protein incorporation and orientation in HSLBs formed by the rupture of proteoliposomes constructed using CFPS of MscL-GFP in the presence of hybrid vesicles. (A) Schematic representation of the vesicle rupture process and resultant orientation of MscL-GFP. (B) Representative MscL-GFP signals in 25 mol % diblock copolymer HSLB before and after TEV protease treatment imaged using TIRF microscopy (scale bar 10 μm). (C) Quantification of MscL-GFP cleavage for all compositions tested. The relative decrease in counted fluorescent punctate particles before and after TEV protease treatment indicates that MscL-GFP in HSLBs was easily accessible (oriented away from the substrate).

but in this particular construct, the expression of GFP is a known reporter of proper protein folding.⁴⁴

To ensure that the HSLBs containing protein both ruptured and remained fluid, we incubated the samples with a membrane-intercalating dye, R18, and carried out FRAP experiments for all of the mobile polymer compositions, up to 35 mol % diblock copolymer. In Figure 3, we compare the diffusion coefficients relative to the diffusion of 0 mol % diblock copolymer HSLBs without protein and mobile fractions of the lipids with and without expressed protein, and we observe no appreciable change in the lipid response. This is expected, as the expression level of protein is kept low to ensure that we can track the proteins to determine their mobility in later experiments. We also learn from this experiment that the proteoliposomes are able to rupture and form planar bilayers at these compositions as we observe full recovery, just as observed above. Images of recovery of the bilayers tested are shown in Figure S4, Supporting Information.

Next, we sought to determine protein orientation in our HSLBs. We used a fluorescence-based cleavage assay to determine the orientation of MscL-GFP after rupturing the hybrid vesicles containing cell-free expressed protein. MscL is expressed as a fusion protein with GFP connected by a TEV cleavage sequence, which can be cleaved by TEV protease. If the protein inserts from the external surface of the membrane, GFP is expected to be oriented toward the outside of the vesicles in solution. If the vesicles rupture on the solid support like "parachutes" with the outside leaflet facing up and the inside facing the support, the GFP should be oriented on the upper leaflet of the HSLB, facing the bulk solution. An illustration of this transition from vesicle to HSLB is shown in Figure 4A. If this is the case, where GFP is outward facing, upon TEV treatment, GFP will be cleaved and diffuse away from the HSLB into the bulk solution. If GFP is oriented facing the support, the TEV recognition sequence will be

inaccessible to the enzyme and GFP should remain located there after treatment.

We used TIRF microscopy of GFP to determine protein orientation on our HSLBs using this TEV cleavage assay. The cleavage of the available fluorescent domain, i.e., GFP, by TEV protease resulted in the loss of fluorescent signal in HSLBs after all cleaved GFP portions were rinsed away, as depicted for 25 mol % diblock copolymer in Figure 4B. Images for all compositions tested are shown in Figure S5 in the Supporting Information. All punctate fluorescent particles were counted before and after TEV treatment to quantify the change, as seen in Figure 4C. We observed that nearly 90% of expressed GFP is cleaved by the protease treatment and MscL-GFP, therefore, exhibits a predominantly unidirectional "upward" orientation in HSLBs. We hypothesize that the few particles that remain are likely due to unruptured vesicles on the surface of the glass or from protein that might have folded in a way that the TEV cleavage site is not easily accessible against the glass support, both of which represent less than roughly 10% of all synthesized proteins. The spontaneous rupture of hybrid vesicles containing cell-free expressed transmembrane proteins demonstrates the integration of membrane proteins into a HSLB with conserved orientation. This first approach relies on the self-assembly of HSLBs from the vesicles fusion method, which provides advantages when wanting to coat a surface of complicated or inaccessible geometries with proteinaceous HSLBs, for example, the interior of microfluidic channels. These observations also suggest that the presence of the diblock copolymer does not change the resultant orientation of MscL-GFP after bilayer formation.

Approach 2: Direct Translation of Proteins into Hybrid-Supported Lipid Bilayers Serves as Another Technique to Form Protein-Containing Supported Bilayers with Controlled Protein Orientation. To make our expression platform more widely applicable, we investigated the cotranslational insertion of MscL-GFP into a preformed HSLB. The vesicle fusion method is typically

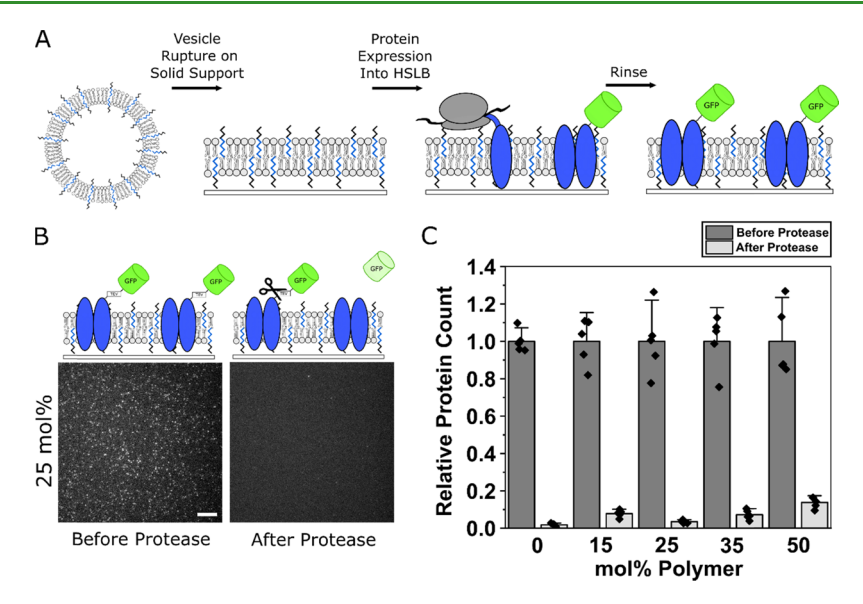


Figure 5. Characterization of protein incorporation and orientation in HSLBs formed by the direct CFPS of MscL-GFP into a preformed HSLB. (A) Schematic of cell-free cotranslational insertion of protein directly into a preformed HSLB and its resultant orientation. (B) Representative MscL-GFP signals in a 25 mol % polymer HSLB before and after TEV protease treatment (scale bar 10 μ m). (C) Quantification of MscL-GFP protein cleavage. The relative decrease in counted fluorescent punctate particles before and after TEV protease treatment. The signal drops indicate MscL-GFP in HSLBs was easily accessible (oriented away from the substrate).

limited to hydrophilic substrates, like glass, so enabling proteins to be synthesized after HSLB formation would unlock more diverse substrates where bilayer formation proceeds in other ways. Unlike synthesis into a vesicle, a potential complication of this strategy is that the nascent peptide chain may interact with the supporting surface and prevent protein expression or folding due to the proximity of the surface. To explore this, we first formed hybrid-supported lipid bilayers containing the same range of lipid-to-diblock copolymer ratios as in our first approach and then synthesized MscL-GFP directly into the HSLB. Bilayers were formed from protein-free vesicles, and excess vesicles were rinsed away before adding the cell-free reaction mixture above the adsorbed bilayer. We let the reaction proceed over the HSLB, allowing proteins to insert and fold into the supported membrane as they were synthesized, as depicted in Figure 5A. Reaction times were determined empirically by monitoring GFP fluorescence over time. We allowed the reaction to proceed to a point where we could discriminate individual fluorescence points using TIRF microscopy and then rinsed away unreacted materials to stop the reaction.

After protein was expressed into preformed supported bilayers containing increasing amounts of diblock copolymer, we found that each HSLB composition provides punctate fluorescence spots, indicating that protein expression and insertion is occurring directly into the supported bilayers (Figure S5, Supporting Information). After determining the number of particles for each sample, we added TEV protease and let the enzyme cleave the exposed GFP molecules from the membrane-bound MscL region. We then rinsed each of the samples to remove cleaved GFP and imaged each sample again, as shown for 25 mol % diblock copolymer in Figure 5B. Each composition tested can be seen in Figure S5, Supporting Information. After counting individual proteins left after the protease treatment and comparing them to the initial protein counts, we observed again that nearly all GFP is cleaved, as quantified in Figure 5C. As with approach 1, this result indicates that essentially all of the protein inserted into the

membrane is oriented uniformly and unidirectionally away from the support. However, comparing the two approaches, cotranslation of protein into a preformed HSLB leads to slightly better protein orientation, about 95 vs 90%. HSLBs with 50 mol % diblock copolymer have slightly more GFP fluorescence relative to compositions with the less diblock copolymer, which we hypothesize is due to some steric hindrance from the high percentage of diblock copolymer blocking access by TEV protease. This second approach is more versatile because this protein expression and integration approach can potentially be used with HSLBs formed by any means (beyond vesicle fusion, e.g., Langmuir-Blodgett-Schaeffer, solvent-assisted bilayer formation, etc.), making this technique advantageous for coating surfaces with lipid compositions incompatible with vesicle fusion, but requiring the presentation of proteins in a membrane environment. 13,4

Diblock Copolymers Enhance the Mobility of Cotranslationally Inserted Membrane Proteins in HSLBS. Once we incorporated MscL-GFP into HSLBs and identified the orientation, we investigated whether the HSLB could maintain protein mobility using single-particle tracking techniques. Conveniently, the GFP tag on the protein can be used to track its movement in the HSLB over time, which enabled us to quantify mobility by calculating local diffusion coefficients and mobile fractions. We analyzed protein motion for both protein incorporation approaches and observed similar results.

For either approach, we observed no protein mobility in 0% diblock copolymer, which is not suprising because there is little space between the SLB and the supporting surface. Similarly, 15 mol % diblock copolymer resulted in only one or two single proteins exhibiting any motion in both approaches. However, at 25 and 35 mol % diblock copolymer concentrations, a significant number of proteins were mobile in both approaches. At 50 mol % diblock copolymer, the vesicle fusion approach did not result in mobile proteins, but the direct expression into preformed HSLBs did. Representative images of expressed, diffusive proteins and trajectories are shown in Figure 6A,B for

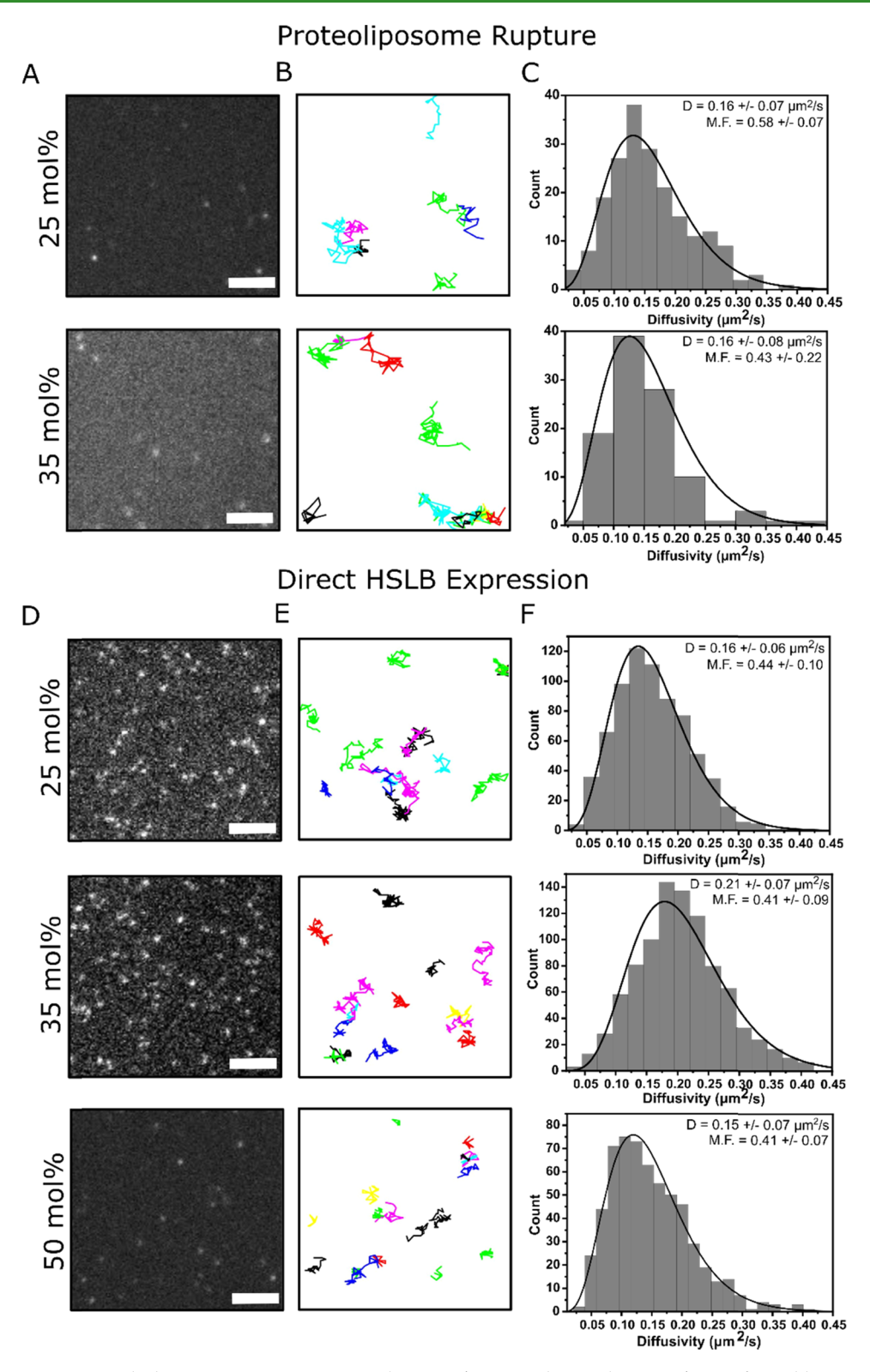


Figure 6. MscL-GFP proteins tracked in HSLBs containing 25 mol % PEO-b-PBD and 35 mol % PEO-b-PBD formed by protein expression into hybrid vesicles or 25–50 mol % PEO-b-PBD formed by direct insertion into a preformed HSLB. (A) Representative TIRF image of MscL-GFP in HSLB. (B) Representative trajectories of MscL-GFP diffusion in the HSLB. (C) Diffusion coefficient histograms for MscL-GFP-tracking experiments along with calculated diffusivities and mobile fraction fit to a γ distribution. (D–F) Corresponding figures for direct HSLB expression (scale bar 5 μ m).

the vesicle-based reaction and Figure 6D,E for the direct expression into the HSLB. We collected the trajectories of individual MscL-GFP molecules and plotted mean square displacements (MSD) as a function of time to determine

diffusion coefficients and protein confinement. Representative MSD measurements over time for all compositions with mobile proteins are shown in Figure S6, Supporting Information. For normal diffusion, the MSD plot as a function

of time gives a straight line with the slope proportional to the diffusion coefficient. We often observed curved plots, which indicates possible confinement effects due to the diblock copolymer in these HSLBs. Therefore, we used the initial slope of the first three time points to determine the local homogeneous diffusion constant. ^{37,42,46,47}

By performing single-particle tracking analysis, we were able to calculate the mobile fraction and mean square displacement (MSD) and fit a gamma distribution to identify the average diffusivity of mobile proteins in HSLBs as seen in Figure 6C,F. Based on the distribution of mobile MscL-GFP molecules, we fit a gamma distribution to calculate the average diffusivity and standard deviation. The calculated diffusivity in the 25 and 35% diblock copolymer HSLBs is 0.16 ± 0.07 and 0.16 ± 0.08 μ m²/s for approach #1 (vesicle fusion), and 0.16 \pm 0.06 and $0.21 \pm 0.07 \ \mu \text{m}^2/\text{s}$ for approach #2 (direct synthesis into HSLB), respectively. The 50 mol % diblock copolymer formed by direct expression has proteins with a diffusivity of 0.15 \pm 0.07 μ m²/s. The mobile fraction in each sample is roughly 0.4–0.6. Among our tested conditions, either direct translation into a HSLB or the vesicle fusion using 25-35 mol % diblock copolymer provides a good quality membrane with unidirectional protein orientation, protein mobility in its local membrane area, and long-range lipid diffusion. The benefit of the diblock copolymer is potentially explained by the fact that hydrophilic PEO units in the diblock copolymer provide cushioning from the glass surface, which presumably prevents interaction and denaturation of MscL-GFP against the glass support, as is observed in the lack of protein mobility in the DOPC-only SLB.⁴⁸ From our conditions, it appears that at least 25 mol % diblock copolymer is required to receive this fluidizing effect.

The protein diffusivity we observed is lower than has been previously reported for similar-sized membrane proteins in SLBs that were formed by more traditional methods involving protein reconstitution or native cellular material.^{37,} However, we included diblock copolymers in our HSLBs, and we observed that the lipid diffusivity dropped with an increasing amount of polymer, which may explain a reduction in overall protein mobility. We note that protein mobility was only observed at 25 mol % polymer and above, and we observed protein mobility between 40 and 60%, which is on par with similar PEGylated lipid systems.³⁷ Longer hydrophilic regions may provide a larger cushion space, which could further increase diffusivity and provide a larger mobile fraction. However, there is a tradeoff: longer-chain polymersomes are harder to rupture into HSLBs and they may decrease protein synthesis as the longer-chain length becomes a steric barrier to cotranslational insertion.

Though lipid diffusion drops significantly with increasing polymer content, we observed that proteins expressed into hybrid vesicles containing 25 and 35 mol % diblock copolymer or directly into a preformed HSLB containing 25, 35, and 50 mol % diblock copolymer were mobile. All compositions had about the same local diffusion coefficients (Figure 7A). This may not be surprising given that we extrapolated the diffusion coefficient from the first three data points of the MSD curve and report here the average value from the associated distribution. In this region, we are likely interrogating a homogeneous local environment. To try to gain more insight into the impact of the polymer, we examined the shape of the trajectories. In most cases, the trajectories were curved, indicating that the proteins were in a confined environment.³⁸

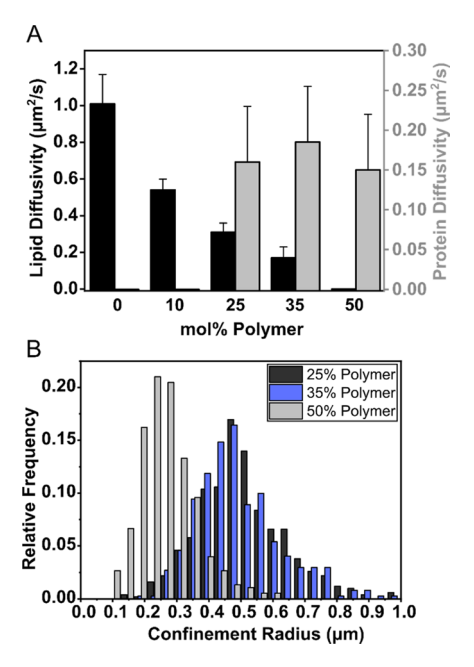


Figure 7. (A) Comparison of lipid and protein diffusivity from 0 to 50 mol % diblock copolymer using approach 2, direct expression. The lipid diffusivity is a maximum at 0 mol % and then decreases with an increase in diblock copolymer concentration. Protein diffusivity is achieved in a minimum of 25 mol % diblock copolymer. Protein diffusivity measurements represent the average *D* obtained from the overall distribution. (B) Calculated confinement radius of diffusive MscL-GFP for 25–50 mol % diblock copolymer formed by direct expression into a preformed HSLB. The confinement radius for 25 and 35 mol % diblock copolymer exhibits similar behavior. HSLBs containing 50 mol % diblock copolymer have proteins with a confinement radius nearly half of the other samples.

To see how this confinement varied with mol % polymer, we calculated the confinement radius, equal to the square root of the max displacement, of the protein introduced through direct expression (Figure 7B). We observe that the average confinement radius for 25 and 35 mol % diblock copolymer is about 450 nm and drops to about 200 nm for 50 mol % diblock copolymer. Interestingly, the average 50 mol % confinement is about the dimension of a vesicle itself and may correspond to protein inserting into intact vesicles on the surface and diffusing within them at this mol %, since we also do not see any lipid diffusion at this mol % by FRAP. On the other side, we see no protein mobility at 0 or 15 mol % diblock copolymer, indicating that the proteins in these bilayers may be inadequately cushioned and stuck to the support. In the range of 25-35 mol % diblock copolymer, there appears to be an optimal composition with enough cushioning to fluidize about 60% of the proteins, but these proteins may be diffusing in a heterogeneous bilayer made of polymer corrals with a radius of

An alternative hypothesis could be that proteins may not be inserted properly but rather be adsorbed on top of the membrane and diffusing there. We have two pieces of evidence to discount this possibility. First, the folding reporter should only fluoresce with proper folding, providing the support that the protein is inserted into the membrane correctly. Because we track proteins that are fluorescent, we are, by definition, tracking only those that are expected to be folded properly. In a second experiment, we sought to determine if the MscL protein was not only properly folded, but in its fully assembled,

homopentamer state.⁵⁰ To determine the MscL oligomeric state, we used single-molecule bleach step analysis to count the number of subunits of the protein complexes in the field of view for 25% diblock copolymer HSLBs. Subunit counting relies on the detection of the individual bleach steps of fluorescently tagged proteins-of-interest. 40,51 For oligomeric protein complexes such as MscL, if all of the fluorescently tagged subunits were fluorescent, the number of photobleaching steps would be equal to the number of subunits per protein complex. However, fluorescent proteins such as GFP can improperly fold and be nonfluorescent, reducing the number of bleach steps observed. Although the fraction of misfolded dark proteins can vary with conditions, it is typically \sim 20–25% of the total. By assuming a value for the fluorescent fraction (77% of our data), the bleach step histogram can be corrected for "missed" subunits. 40 Our corrected bleach step histogram shows that a number of MscL-GFP protein complexes in the bilayer displayed five discrete bleaching steps (Figure 8). Although we did observe populations of

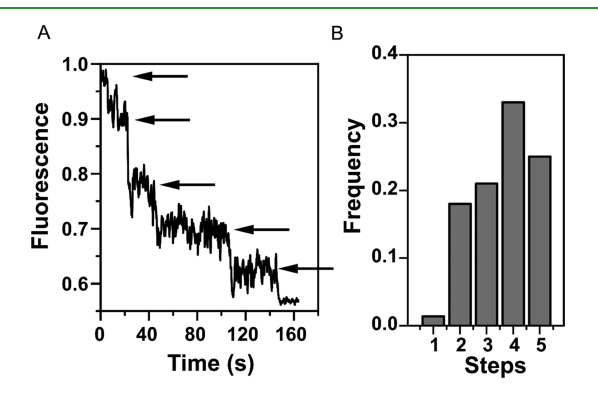


Figure 8. Subunit photobleaching experiment of MscL-GFP in 25% diblock copolymer HSLB. (A) Representative intensity—time trace of the photobleaching steps observed for MscL-GFP. Five photobleaching steps are denoted by arrow marks. (B) Histogram of the number of photobleaching steps from the intensity—time trace and fitted to binomial distribution for a total of n = 350 spots.

smaller oligomers, with tetramers being the largest fraction, this is typically seen due to bleach steps occurring too close in time to accurately separate and to bleaching that can occur during focusing and locating the field of view. Based on these results, we believe that the majority of cell-free synthesized MscL-GFPs oligomerize as pentamers in our system, validating the applicability for conducting single-molecule studies. Thus, we can conclude that the proteins we observe in the HSLBs made with moderate amounts of diblock copolymer are folded, inserted, in a native pentameric form, and able to diffuse within an apparently confined bilayer environment.

Incorporation of Diblock Copolymer Creates HSLBs with Tunable Protein and Lipid Properties. The versatility of these approaches in creating proteinaceous bilayers offers flexibility in many ways that should open this technology to new applications. Proteins that may not insert efficiently into a flat membrane surface may benefit from the vesicle-based method in the first approach, and membrane compositions that are not compatible with vesicle fusion to form a supported bilayer may benefit from the second approach using a direct expression of protein into them after the bilayer is formed. In terms of lipid mobility, certain studies may be assisted by slower diffusion with a high mobile fraction

to better regulate or slow down biological processes under study. Incorporating diblock copolymers can achieve this without changing the underlying lipid composition. Furthermore, given that protein mobility is an important property for many membrane processes, being able to preserve this aspect in this platform should open the door to many exciting applications of this cell-free approach of creating a biomimetic proteinaceous membrane surfaces. For example, binding assays with small molecules, proteins, antibodies, and viral particles among others, rely on multivalent interactions with membrane species that result from in-plane, lateral motion. Another example was illustrated here, examining protein subunit oligomerization required for ion channel formation, another important biological phenomenon dependent on membrane mobility. In the future, HSLBs could be used to study membrane protein function more easily than in a live cell or other complex system, since the protein expression levels and membrane properties can be controlled.

CONCLUSIONS

We have demonstrated, for the first time, the assembly of HSLBs constructed from phospholipids and diblock copolymers with transmembrane proteins that mimic native biological behavior. Here, we showed that planar, supported bilayers could be assembled from phospholipids and diblock copolymers and that mobile, oriented membrane proteins could be integrated using cell-free synthesis methods. We demonstrated that a GFP-labeled ion channel, MscL-GFP, could be incorporated into HSLBs by two different approaches: (1) We first expressed MscL-GFP into vesicles and showed using a protease cleavage assay that proteoliposomes can form HSLBs and maintain the orientation of integrated MscL-GFP after rupture. (2) We showed that MscL-GFP could be integrated into HSLBs after formation by incubating a cell-free reaction with the preformed HSLBs. Our findings indicate that CFPS provides a potentially powerful strategy to assemble planar lipid platforms with mobile, oriented biological proteins.

The ability to synthesize proteins directly into a supported membrane without the need for cell culture or protein purification provides a powerful tool in biotechnology applications. This approach is expected to be compatible with various SLB fabrication methods, opening this new way to incorporate membrane proteins into tunable SLBs using cellfree expression methods. A critical finding of this study is that the inclusion of small amounts of a diblock copolymer into HSLBs facilitated the mobility of the integrated membrane proteins. Hence, we anticipate that the combination of CFPS and hybrid SLB platforms to integrate membrane proteins in model membranes will provide a wide breadth of interesting uses in biophysical studies and technological applications, such as membrane protein biosensors. Because of the easily tunable properties and the maintenance of native biological features, in the future, cell-free membrane protein functionalized SLB platforms can be used to address a number of central challenges such as membrane transport phenomena, screening of therapeutically relevant membrane proteins, or complex binding events from a range of targets, on nearly any surface.

ASSOCIATED CONTENT

Supporting Information

The Supporting Information is available free of charge at https://pubs.acs.org/doi/10.1021/acsabm.0c01482.

Characterization of hybrid vesicles: intensity-size distribution histogram, diameter, and ζ potential of vesicles consisting of DOPC and PEO-b-PBD; HSLBs have two-dimensional fluidity: FRAP images, line scans across the photobleaching spot and recovery curve using TR-DHPE as fluorophore; QCM-D analysis: frequency and dissipation change as a function of time; FRAP images of HSLBs with and without expressed MscL-GFP; protease orientation assay for HSLBs formed by vesicle fusion and direct expression; and mean square displacement plots for mobile proteins in HSLBs (PDF)

AUTHOR INFORMATION

Corresponding Authors

Neha P. Kamat — Department of Biomedical Engineering and Center for Synthetic Biology, Northwestern University, Evanston, Illinois 60208, United States; orcid.org/0000-0001-9362-6106; Email: nkamat@northwestern.edu

Susan Daniel — R.F. School of Chemical and Biomolecular Engineering, Cornell University, Ithaca, New York 14853, United States; o orcid.org/0000-0001-7773-0835; Email: sd386@cornell.edu

Authors

Zachary A. Manzer — R.F. School of Chemical and Biomolecular Engineering, Cornell University, Ithaca, New York 14853, United States; orcid.org/0000-0002-8225-8990

Surajit Ghosh – R.F. School of Chemical and Biomolecular Engineering, Cornell University, Ithaca, New York 14853, United States

Miranda L. Jacobs — Department of Biomedical Engineering and Interdisciplinary Biological Sciences Program, Northwestern University, Evanston, Illinois 60208, United States

Srinivasan Krishnan – Boyce Thompson Institute, Ithaca, New York 14853, United States

Warren R. Zipfel – Meinig School of Biomedical Engineering, Cornell University, Ithaca, New York 14853, United States

Miguel Piñeros — School of Integrative Plant Science, Cornell University, Ithaca, New York 14853, United States; Boyce Thompson Institute, Ithaca, New York 14853, United States; Robert W. Holley Center for Agriculture and Health, US Department of Agriculture—Agricultural Research Service, Ithaca, New York 14853, United States

Complete contact information is available at: https://pubs.acs.org/10.1021/acsabm.0c01482

Author Contributions

Z.A.M. and S.G. contributed equally to this work. The manuscript was written through the contributions of all authors. All authors have given approval to the final version of the manuscript. Z.A.M., S.G., M.L.J., N.P.K., and S.D. conceptualized the project and edited the manuscript. Z.A.M., S.G., and S.D. drafted the manuscript. Z.A.M. and S.G. conducted experiments and analyzed the data. S.K., W.R.Z., and M.P. conducted the subunit photobleaching experiments.

Notes

The authors declare no competing financial interest.

ACKNOWLEDGMENTS

This work was supported by the NSF grant MCB-1935356 (S.D. and N.P.K.), Air Force Office of Scientific Research (AFOSR) YIP FA9550-19-1-0039 P00001 (N.P.K.), NSF grant CBET-1844219 (N.P.K.), and the Searle Funds at The Chicago Community Trust (N.P.K.). M.L.J. is supported by an American Heart Association Predoctoral Fellowship Grant no. 20PRE35180215 and AFOSR grant FA9550-19-1-0039 P00001 to N.P.K. The project described was supported by T32GM008500 from the National Institute of General Medical Sciences (Z.A.M.). The content is solely the responsibility of the authors and does not necessarily represent the official views of the National Institute of General Medical Sciences or the National Institutes of Health. S.D. acknowledges funding for this project, sponsored by the Defense Advanced Research Projects Agency (DARPA) Army Research Office and accomplished under Cooperative Agreement Number W911NF-18-2-0152. The views and conclusions contained in this document are those of the authors and should not be interpreted as representing the official policies, either expressed or implied, of DARPA or the Army Research Office or the U.S. Government. The U.S. Government is authorized to reproduce and distribute reprints for Government purposes notwithstanding any copyright notation herein.

REFERENCES

- (1) Peetla, C.; Bhave, R.; Vijayaraghavalu, S.; Stine, A.; Kooijman, E.; Labhasetwar, V. Drug Resistance in Breast Cancer Cells: Biophysical Characterization of and Doxorubicin Interactions with Membrane Lipids. *Mol. Pharmaceutics* **2010**, *7*, 2334–2348.
- (2) Misawa, N.; Osaki, T.; Takeuchi, S. Membrane Protein-Based Biosensors. J. R. Soc. Interface 2018, 15, No. 20170952.
- (3) Bally, M.; Bailey, K.; Sugihara, K.; Grieshaber, D.; Vörös, J.; Stäler, B. Liposome and Lipid Bilayer Arrays towards Biosensing Applications. *Small* **2010**, *6*, 2481–2497.
- (4) Liu, H. Y.; Pappa, A. M.; Pavia, A.; Pitsalidis, C.; Thiburce, Q.; Salleo, A.; Owens, R. M.; Daniel, S. Self-Assembly of Mammalian-Cell Membranes on Bioelectronic Devices with Functional Transmembrane Proteins. *Langmuir* **2020**, *36*, 7325–7331.
- (5) Pappa, A.-M.; Liu, H.-Y.; Traberg-Christensen, W.; Thiburce, Q.; Savva, A.; Pavia, A.; Salleo, A.; Daniel, S.; Owens, R. M. Optical and Electronic Ion Channel Monitoring from Native Human Membranes. ACS Nano 2020, 14, 12538–12545.
- (6) Shi, J.; Yang, T.; Cremer, P. S. Multiplexing Ligand-Receptor Binding Measurements by Chemically Patterning Microfluidic Channels. *Anal. Chem.* **2008**, *80*, 6078–6084.
- (7) Costello, D. A.; Millet, J. K.; Hsia, C. Y.; Whittaker, G. R.; Daniel, S. Single Particle Assay of Coronavirus Membrane Fusion with Proteinaceous Receptor-Embedded Supported Bilayers. *Biomaterials* **2013**, *34*, 7895–7904.
- (8) Zeno, W. F.; Johnson, K. E.; Sasaki, D. Y.; Risbud, S. H.; Longo, M. L. Dynamics of Crowding-Induced Mixing in Phase Separated Lipid Bilayers. *J. Phys. Chem. B* **2016**, *120*, 11180–11190.
- (9) Richter, R. P.; Brisson, A. R. Following the Formation of Supported Lipid Bilayers on Mica: A Study Combining AFM, QCM-D, and Ellipsometry. *Biophys. J.* **2005**, *88*, 3422–3433.
- (10) Lee, T.-H.; Hirst, D. J.; Kulkarni, K.; Del Borgo, M. P.; Aguilar, M.-I. Exploring Molecular-Biomembrane Interactions with Surface Plasmon Resonance and Dual Polarization Interferometry Technology: Expanding the Spotlight onto Biomembrane Structure. *Chem. Rev.* 2018, 118, 5392–5487.
- (11) Richter, R. P.; Escarpit, R. R.; Cedex, P. Formation of Solid-Supported Lipid Bilayers: An Integrated View. *Langmuir* **2006**, *22*, 3497–3505.
- (12) Tamm, L. K.; McConnell, H. M. Supported Phospholipid Bilayers. *Biophys. J.* **1985**, 47, 105–113.

- (13) Jackman, J. A.; Cho, N. Supported Lipid Bilayer Formation: Beyond Vesicle Fusion. *Langmuir* **2020**, *36*, 1387–1400.
- (14) Richter, R. P.; Brisson, A. R. Following the Formation of Supported Lipid Bilayers on Mica: A Study Combining AFM, QCM-D, and Ellipsometry. *Biophys. J.* **2005**, *88*, 3422–3433.
- (15) Cho, N.; Frank, C. W.; Kasemo, B.; Höök, F. Quartz Crystal Microbalance with Dissipation Monitoring of Supported Lipid Bilayers on Various Substrates. *Nat. Protoc.* **2010**, *5*, 1096–1106.
- (16) Fonseka, N. M.; Liang, B.; Orosz, K. S.; Jones, I. W.; Hall, H. K.; Christie, H. S.; Aspinwall, C. A.; Saavedra, S. S. Nanodomain Formation in Planar Supported Lipid Bilayers Composed of Fluid and Polymerized Dienoyl Lipids. *Langmuir* **2019**, *35*, 12483–12491.
- (17) Glazier, R.; Salaita, K. Supported Lipid Bilayer Platforms to Probe Cell Mechanobiology. *Biochim. Biophys. Acta, Biomembr.* **2017**, 1859, 1465–1482.
- (18) Castellana, E. T.; Cremer, P. S. Solid Supported Lipid Bilayers: From Biophysical Studies to Sensor Design. *Surf. Sci. Rep.* **2006**, *61*, 429–444.
- (19) Hsia, C. Y.; Richards, M. J.; Daniel, S. A Review of Traditional and Emerging Methods to Characterize Lipid-Protein Interactions in Biological Membranes. *Anal. Methods* **2015**, *7*, 7076–7094.
- (20) Shimizu, Y.; Inoue, A.; Tomari, Y.; Suzuki, T.; Yokogawa, T.; Nishikawa, K.; Ueda, T. Cell-Free Translation Reconstituted with Purified Components. *Nat. Biotechnol.* **2001**, *19*, 751–755.
- (21) Jewett, M. C.; Calhoun, K. A.; Voloshin, A.; Wuu, J. J.; Swartz, J. R. An Integrated Cell-Free Metabolic Platform for Protein Production and Synthetic Biology. *Mol. Syst. Biol.* **2008**, *4*, No. 220.
- (22) Zieleniecki, J. L.; Nagarajan, Y.; Waters, S.; Rongala, J.; Thompson, V.; Hrmova, M.; Köper, I. Cell-Free Synthesis of a Functional Membrane Transporter into a Tethered Bilayer Lipid Membrane. *Langmuir* **2016**, *32*, 2445–2449.
- (23) Soranzo, T.; Martin, D. K.; Lenormand, J. L.; Watkins, E. B. Coupling Neutron Reflectivity with Cell-Free Protein Synthesis to Probe Membrane Protein Structure in Supported Bilayers. *Sci. Rep.* **2017**, *7*, No. 3399.
- (24) Sachse, R.; Dondapati, S. K.; Fenz, S. F.; Schmidt, T.; Kubick, S. Membrane Protein Synthesis in Cell-Free Systems: From Bio-Mimetic Systems to Bio-Membranes. *FEBS Lett.* **2014**, *588*, 2774–2781.
- (25) Jacobs, M. L.; Boyd, M. A.; Kamat, N. P. Diblock Copolymers Enhance Folding of a Mechanosensitive Membrane Protein during Cell-Free Expression. *Proc. Natl. Acad. Sci. U.S.A.* **2019**, *116*, 4031–4036.
- (26) Nallani, M.; Andreasson-Ochsner, M.; Tan, C.-W. D.; Sinner, E.-K.; Wisantoso, Y.; Geifman-Shochat, S.; Hunziker, W. Proteopolymersomes: In Vitro Production of a Membrane Protein in Polymersome Membranes. *Biointerphases* **2011**, *6*, 153–157.
- (27) Arslan Yildiz, A.; Kang, C.; Sinner, E. K. Biomimetic Membrane Platform Containing HERG Potassium Channel and Its Application to Drug Screening. *Analyst* **2013**, *138*, 2007–2012.
- (28) May, S.; Andreasson-Ochsner, M.; Fu, Z.; Low, Y. X.; Tan, D.; De Hoog, H. P. M.; Ritz, S.; Nallani, M.; Sinner, E. K. In Vitro Expressed GPCR Inserted in Polymersome Membranes for Ligand-Binding Studies. *Angew. Chem., Int. Ed.* **2013**, *52*, 749–753.
- (29) Zapf, T.; Tan, C. W. D.; Reinelt, T.; Huber, C.; Shaohua, D.; Geifman-Shochat, S.; Paulsen, H.; Sinner, E. K. Synthesis and Functional Reconstitution of Light-Harvesting Complex II into Polymeric Membrane Architectures. *Angew. Chem., Int. Ed.* **2015**, 54, 14664–14668.
- (30) Andreasson-Ochsner, M.; Fu, Z.; May, S.; Ying Xiu, L.; Nallani, M.; Sinner, E. K. Selective Deposition and Self-Assembly of Triblock Copolymers into Matrix Arrays for Membrane Protein Production. *Langmuir* **2012**, *28*, 2044–2048.
- (31) Gettel, D. L.; Sanborn, J.; Patel, M. A.; de Hoog, H.; Liedberg, B.; Nallani, M.; Parikh, A. N. Mixing, Diffusion, and Percolation in Binary Supported Membranes Containing Mixtures of Lipids and Amphiphilic Block Copolymers. *J. Am. Chem. Soc.* **2014**, *136*, 10186–10189.

- (32) Mumtaz Virk, M.; Hofmann, B.; Reimhult, E. Formation and Characteristics of Lipid-Blended Block Copolymer Bilayers on a Solid Support Investigated by Quartz Crystal Microbalance and Atomic Force Microscopy. *Langmuir* **2019**, *35*, 739–749.
- (33) Paxton, W. F.; McAninch, P. T.; Shin, S. H. R.; Brumbach, M. T. Adsorption and Fusion of Hybrid Lipid/Polymer Vesicles onto 2D and 3D Surfaces. *Soft Matter* **2018**, *14*, 8112–8118.
- (34) Kamat, N. P.; Robbins, G. P.; Rawson, J.; Therien, M. J.; Dmochowski, I. J.; Hammer, D. A. A Generalized System for Photoresponsive Membrane Rupture in Polymersomes. *Adv. Funct. Mater.* **2010**, 20, 2588–2596.
- (35) Soumpasis, D. M. Theoretical Analysis of Fluorescence Photobleaching Recovery Experiments. *Biophys. J.* **1983**, *41*, 95–97.
- (36) Schneider, C. A.; Rasband, W. S.; Eliceiri, K. W. NIH Image to Image]: 25 Years of Image Analysis. *Nat. Methods* **2012**, *9*, 671–675.
- (37) Richards, M. J.; Hsia, C. Y.; Singh, R. R.; Haider, H.; Kumpf, J.; Kawate, T.; Daniel, S. Membrane Protein Mobility and Orientation Preserved in Supported Bilayers Created Directly from Cell Plasma Membrane Blebs. *Langmuir* **2016**, 32, 2963–2974.
- (38) Saxton, M. J.; Jacobson, K. Single-Particle Tracking: Applications to Membrane Dynamics. *Annu. Rev. Biophys. Biomol. Struct.* **1997**, *26*, 373–399.
- (39) Jin, S.; Haggie, P. M.; Verkman, A. S. Single-Particle Tracking of Membrane Protein Diffusion in a Potential: Simulation, Detection, and Application to Confined Diffusion of CFTR Cl Channels. *Biophys. J.* **2007**, *93*, 1079–1088.
- (40) Singh, A.; Van Slyke, A. L.; Sirenko, M.; Song, A.; Kammermeier, P. J.; Zipfel, W. R. Stoichiometric Analysis of Protein Complexes by Cell Fusion and Single Molecule Imaging. *Sci. Rep.* **2020**, *10*, No. 14866.
- (41) Diaz, A. J.; Albertorio, F.; Daniel, S.; Cremer, P. S. Double Cushions Preserve Transmembrane Protein Mobility in Supported Bilayer Systems. *Langmuir* **2008**, *24*, 6820–6826.
- (42) Liu, H. Y.; Chen, W. L.; Ober, C. K.; Daniel, S. Biologically Complex Planar Cell Plasma Membranes Supported on Polyelectrolyte Cushions Enhance Transmembrane Protein Mobility and Retain Native Orientation. *Langmuir* **2018**, 34, 1061–1072.
- (43) Bermúdez, H.; Hammer, D. A.; Discher, D. E. Effect of Bilayer Thickness on Membrane Bending Rigidity. *Langmuir* **2004**, *20*, 540–543
- (44) Waldo, G. S.; Standish, B. M.; Berendzen, J.; Terwilliger, T. C. Rapid Protein-Folding Assay Using Green Fluorescent Protein. *Nat. Biotechnol.* **1999**, *17*, 691–695.
- (45) Su, H.; Liu, H.; Pappa, A.; Hidalgo, T. C.; Cavassin, P.; Owens, M.; Daniel, S.; Inal, S. Facile Generation of Biomimetic-Supported Lipid Bilayers on Conducting Polymer Surfaces for Membrane Biosensing. *ACS Appl. Mater. Interfaces* **2019**, *11*, 43799–73810.
- (46) Kusumi, A.; Sako, Y.; Yamamoto, M. Confined Lateral Diffusion of Membrane Receptors as Studied by Single Particle Tracking (Nanovid Microscopy). Effects of Calcium-Induced Differentiation in Cultured Epithelial Cells. *Biophys. J.* 1993, 65, 2021–2040.
- (47) Smith, P. R.; Morrison, I. E. G.; Wilson, K. M.; Fernández, N.; Cherry, R. J. Anomalous Diffusion of Major Histocompatibility Complex Class I Molecules on HeLa Cells Determined by Single Particle Tracking. *Biophys. J.* 1999, 76, 3331–3344.
- (48) de Gennes, P.-G. Scaling Concepts in Polymer Physics; Cornell University Press: Ithaca, NY, 1979.
- (49) Kawate, T.; Michel, J. C.; Birdsong, W. T.; Gouaux, E. Crystal Structure of the ATP-Gated P2X4 Ion Channel in the Closed State. *Nature* **2009**, *460*, 592–598.
- (50) Perozo, E.; Cortes, D. M.; Sompornpisut, P.; Kloda, A.; Martinac, B. Open Channel Structure of MscL and the Gating Mechanism of Mechanosensitive Channels. *Nature* **2002**, *418*, 942–948.
- (51) Ulbrich, M. H.; Isacoff, E. Y. Subunit Counting in Membrane-Bound Proteins. *Nat. Methods* **2007**, *4*, 319–321.